STRAIN-DEPENDENT DAMPING OF PAULOWNIA WOOD AT ROOM TEMPERATURE AND CONSTANT MOISTURE CONTENT

J. GÖKEN[1], N. SABA[2]

[1] University of Applied Sciences Emden/Leer, Faculty of Maritime Sciences, Bergmannstraße 36, 26789 Leer, Germany
Corresponding author, E-mail: juergen.goeken@hs-emden-leer.de
[2] University of Balamand, Faculty of Engineering, Department of Mechanical Engineering, Koura campus, 100 p.o. Box Tripoli, Lebanon
Corresponding author, E-mail: nicolas.saba@balamand.edu.lb

Received July 23, 2024

Abstract. Against the backdrop of global warming and the necessary reduction of CO_2, the material wood is experiencing a renaissance as a result of increasing social acceptance. However, questions of harmless reforestation also come to the forefront. Ultimately, plantation cultivation of wood is unavoidable in order to meet the increasing demand for wood in the coming years. Agroforestry is the focus of economic and technical interest in this regard.

Paulownia or Kiri tree belongs to the Paulowniaceae family and is the tree with the highest growth rate in the world. It has a large leaf area that can absorb correspondingly high amounts of CO_2. Originally from China, it is now planted worldwide and is considered a climate tree. However, it must face the accusation of invasiveness. Therefore, less invasive varieties of Paulownia are of interest. However, these should also have appropriate mechanical properties. One of these material properties is damping, which significantly affects the acoustic behaviour.

In this study, the strain-dependent damping was investigated by measuring the logarithmic decrement of free decaying bending oscillations. The measurements were carried out on a common Paulownia species (obtained from plantations in Georgia, Italy and Spain) and a new species of Paulownia obtained from a plantation in Germany. It is worth mentioning that the new wood variety was harvested for the first time in Germany.

Since damping is strongly influenced by microstructure, which is in turn influenced by site-specific nutrient supply, this study examined how damping behaviour develops with strain and the extent of its variation. It was found that the damping curves exhibited a strain-independent and a strain-dependent area. The bending modulus was calculated from the oscillation frequency and showed that the values range from about 1024 N/mm^2 to 5873 N/mm^2. This large variation appears to stem from the fiber orientation of the tested samples, which also affects the damping values.

Key words: Wood, Bio-based materials, Damping, Dynamic mechanical analysis.

DOI: https://doi.org/10.59277/RomJPhys.2024.69.909

1. INTRODUCTION

Timber sector. Developments in supply and demand as well as production and transport costs are important parameters in the timber sector and are included in the Global Forest Products Model (GFPM). This is an economic model of production, consumption, and trade in forest products at the global level [1]. Another parameter is the Roundwood Equivalent volume (RWE volume) and a measure of the volume of logs (roundwood) used in the manufacture of wood-based products (including wood pulp, paper, wooden furniture, joinery and plywood) [2].

The outlook for primary wood products consumption based on GFPM shows an increase of 0.8 billion m^3 (+ 37 percent) RWE from 2.3 billion m^3 RWE in 2020 to 3.1 billion m^3 RWE in 2050. Wood-based panels may see the strongest increase in future consumption (+ 102 percent for veneer/plywood and + 72 percent for particle/fibre board). Further, the outlook shows an increase of 30 percent in consumption of sawnwood and a moderate 5 percent increase for wood pulp [3].

Climate change and environmental degradation are an existential threat to Europe and the world. To overcome these challenges, the European Green Deal will transform the EU into a modern, resource-efficient and competitive economy [4]. Effective plantation cultivation is essential to meet this global demand. Agroforestry can accompany forward-looking forestry.

Agroforestry is defined as the deliberate combination of woody vegetation with crops and/or animal systems and has been proposed as a suitable method for agricultural management capable of facing the current environmental challenges [5]. There are two main groups of agroforestry that can be further subdivided: a) the use of trees that produce valuable fruits (for human consumption or for animal feed), and b) the use of trees that provide shade for newly planted trees, stabilise soil moisture, produce wood for industry, etc. In the second case, fast-growing species are used that can create the necessary conditions for the supported plantation in a few years. The objectives when using these trees are higher wood yields and shorter harvest cycles [6].

Wood as a natural raw material is particularly environmentally friendly, as long as it comes from sustainably managed forests. The natural cycle of wood begins in forests as trees grow, with solar energy and carbon dioxide (CO_2) as the key inputs for wood formation. Even during growth, the tree actively contributes to climate protection by transforming CO_2 and permanently binding carbon. The cycle continues with harvesting from these forests with the wood being used to produce a broad range of products [7].

A fast-growing timber which demonstrably enables plantation cultivation is Paulownia wood. Paulownia is officially recognised as the fastest growing tree in the world. Its genus includes more than 6 species [8] and has attracted enormous interest from academia and industry in recent years [9]. Paulownia trees originate from China and are also grown throughout Asia, USA, Australia and Europe [10]. Due to the large size of its leaves, one Paulownia tree can absorb daily up to 22 kg of CO_2 and produce approximately 6 kg of O_2. For comparison, over one year a mature tree will take up about 22 kilograms of carbon dioxide from the atmosphere [11]. Depending on the state of environment of Paulownia can attain in a height to a 30 m [12].

This tree, under favourable conditions, can reach up 6-8 metres per year [13]. As an indication of growth rates, reference should be made here, for example, to the results of Erskine *et al.* [14]. In their work the height growth of 16 high-value rainforest tree species was evaluated over a 5-year period under favourable plantation conditions. The fastest grow rate was about 2 metres per year. With Paulownia, a growth of

1 cubic metre is achieved in 7-8 years, which is incomparable with the growth of other fast-growing trees [13].

Paulownia has the botanical and silvical characteristics commonly associated with an invasive species that enable it to establish and spread in disturbed areas [15]. This problem can be reduced by planting Paulownia plantations with trees that produce no seeds. This goal is being pursued with the introduction of a special variety (Paulownia NordMax21®). Paulownia NordMax21® is a German hybrid of Paulownia tomentosa and Paulownia fortunei. The genetic influence of Paulownia tomentosa provides this hybrid breed with particularly wide site tolerance and high frost resistance. The cross-breeding partner, Paulownia fortunei, dominates the straight, robust, and homogeneous stem growth of this variety [16]. Samples of this special variety taken from a German plantation (location: Ladenburg, growing time: 11 to 12 years) are used in this study, with other samples coming from common Paulownia varieties (bred in Italy, Spain and Georgia).

However, there remains lack of mechanical parameters. Without understanding the correlations between structural properties, which can be complex, especially in biological material such as wood, developments in wood utilisation are limited. This is particularly evident when dealing with lesser-known wood species or when, as with the wood samples in this study, the wood species has undergone genetic adaptation to Central European climate conditions. Various measurements are necessary to build up the physical understanding of the wood at hand. As the Paulownia tree is better known worldwide as the Kiri tree, this name will be retained in the following. Some specific properties of Kiri wood are listed in Table 1.

Table 1

Information about Kiri wood [17]

Property	**Description of Kiri wood**
specific density	about 250 kg/m^3; comparison: oak: ~ 770 kg/m^3; beech: ~ 720 kg/m^3; pine ~ 480 kg/m^3; spruce: ~ 450 kg/m^3 → Low weight saves transport and energy costs.
strength	honeycomb-like cell structure → Kiri wood is very strong and stable in relation to its weight.
dimensional stability	extremely low swelling and shrinking behaviour → This makes Kiri wood the first choice in environments with changing humidity levels.
thermal conductivity	only 0.09 W/mK → Kiri wood stores a lot of air in its vacuoles and therefore insulates more than twice as well as oak or beech.
weather-proof	no splitting, no cupping, no warping
knot occurence	completely knot-free assortment is possible → The delicate grain and pleasantly smooth feel make it attractive for different areas of application.
processing	does not splinter, can be easily processed manually and mechanically, can easily absorb glazes and varnishes, and is very good for gluing

Wood is utilised in various areas of life. This also applies to Kiri wood. Some fields of application including concrete examples are shown in Table 2.

Table 2

Application areas of Kiri wood [18]

Mobility	**Construction**	**Lifestyle**
ship and boat construction, surfboards, model and glider airplanes, caravan manufacturing	ceilings, stairs, windows, modular buildings, tiny houses, wooden facades, structures for trade shows, events, and stages	furniture, home accessories such as vases and bowls, garden furniture, packaging and storage containers

As accurately summarised by Mai *et al.* [19], wood physics is an integral part of wood science. It is based on the findings of wood chemistry, wood anatomy and biology as well as classical physics, mechanics and strength of materials.

Important areas of wood physics are: a) the behaviour of wood related to moisture (basics of moisture sorption, swelling and shrinkage), b) the influence of temperature on the wood properties, the heat conduction and the heat storage, and c) the mechanical, rheological and acoustic properties of wood and wood-based materials [19]. Besides the moisture content, the growing conditions at the tree's location also play an important role and significantly determine the mechanical properties [20]. Therefore, it is not surprising that the properties of wood should only be regarded as 'tentative' guidelines. Ultimately, determined property values can only be considered as individual data.

Material damping. Material damping describes the losses in material due to internal friction and originates from the energy dissipation associated with microstructure defects such as chain motion in polymers [21]. In a work of Dunlop [22], the loss mechanism of wood appears to be due to either motions of the absorbed water molecules themselves or to motions of some molecular parts of the wood structure which are affected by the presence of water. Since the parameters time, temperature and moisture content influence the mechanical properties of wood, it is therefore considered viscoelastic [22]. The term 'viscoelasticity' may include both recoverable and non-recoverable behaviour [23].

Viscoelastic materials are those for which the relationship between stress and strain depends on time. A strain response of a linearly viscoelastic material is also sinusoidal in time, but the response will lag the stress [24]. This lag characterises the material damping. Material damping depends on many factors. The most important of these factors are: type of materials, stress amplitude, internal forces, number of cycles, sizes of geometry, quality of surfaces and temperature [25]. For this reason, it is mandatory to precisely specify the experimental conditions for damping measurements.

In this study, the damping behaviour of Kiri wood will be investigated. Since the sample material comes from plantations in different countries and the respective storage or drying conditions are not known, the absolute values are less relevant than the variation in damping values. The results contribute to the knowledge of the acoustic properties of wood [26, 27]. The acoustic properties itself are strongly dependent on the modulus of elasticity and the density of the wood, as shown, for example, in a study by Wegst [28]. Even though the commercially available Kiri wood comes from invasive species of trees (as opposed to the hybrid variety used here), it is considered sustainable. It may be possible to substitute plastic-based insulating material with sustainable Kiri wood. If wood is used as a construction material and possesses a high damping capacity, no additional vibration dampers are necessary. Moreover, wood's low weight compared to metals is of significant importance in the transport sector. Wood also captivates with its high specific strength and elasticity simultaneously [29].

2. EXPERIMENTAL DETAILS

Wooden samples were made from the Kiri tree which originates from plantations in: a) Italy, b) Spain, c) Georgia, and d) Germany. They were used for investigation of the strain-dependent damping. All samples were obtained from wood harvested approximately one year ago. Kiri wood was delivered as boards which were taken in the direction of growth of the tree trunk.

The goal was to machine cut as many samples as possible from these boards. The cutting direction was not necessarily the growth direction of the tree. This resulted in an inconsistent fibre orientation of the samples which were used as bending beams. The designation of the fibre orientations is shown in Fig. 1.

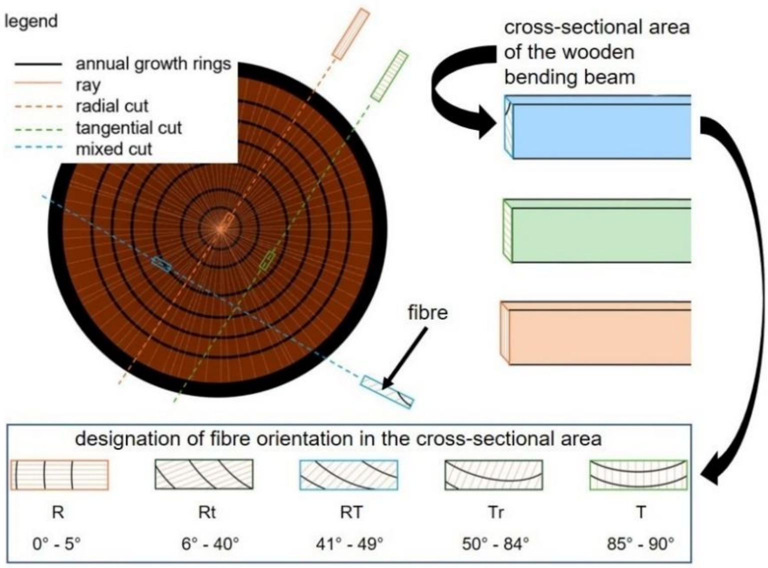

Fig. 1 – Fibre orientations of the bending beams and designation of the fibre orientation. Adopted from Ref. [30] (modified).

The damping measurements were carried out on wooden samples with rectangular shape and the following dimensions (Fig. 2): thickness a about 3 mm, width b of 10 mm and total length l of 120 mm. Damping was measured from freely decaying vibrations of these samples (acting as bending beams) clamped at one side. The effective vibration length of the samples was 85 mm.

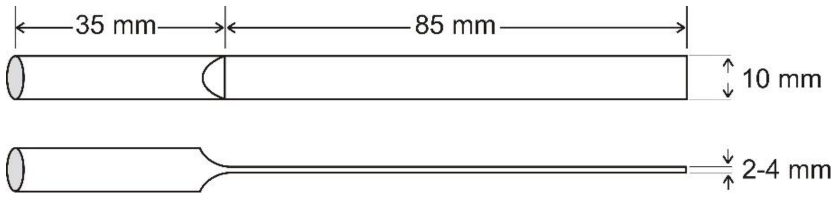

Fig. 2 – Sample form and dimensions.

All measurements were determined at room temperature and constant moisture content (equilibrium moisture content ~ 10%). The moisture content was measured by a pin-type wood moisture meter (Voltcraft® FM-300, Voltcraft®, Hirschau, Germany) which measures the electrical resistance between two plug gauges. These gauges were inserted into the piece of wood. The moisture content ranged from 9.3% to 10% with an accuracy of ± 1% approximately.

The significant influence of temperature and moisture content parameters on the damping behaviour of wood was demonstrated in an own separate study [31]. Without keeping these parameters constant, identifying the inherently complex damping mechanisms in wood are even more difficult.

Measuring procedure. The sample is deflected at the free end (deflection: z') and mechanically excited to oscillate. After excitation, the sample undergoes a free damped harmonic oscillation. According to Fig. 3, the maximum strain ε_{max} is generated near the clamped side of the bending beam, which is used as a reference value for amplitude-dependent damping measurements.

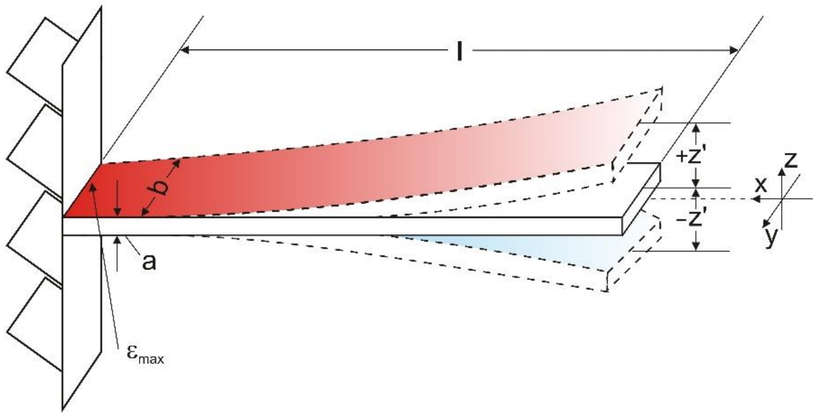

Fig. 3 – Maintaining the maximum strain ε_{max} at mechanical excitation at the free end.

ε_{max} can be calculated as

$$\varepsilon_{max} = \frac{3a}{2l^2} z'. \qquad (1)$$

According to Eq. (1), using a maximum deflection z' thus leads to the amplitude of ε_{max}.

Material damping was measured in terms of the logarithmic decrement δ which is defined by (*e.g.* Ref. [32])

$$\delta = \frac{1}{k} \ln\left(\frac{A_n}{A_{n+k}}\right) \qquad (2)$$

and represents the measure of the rate of decay in vibration amplitude of a harmonically decaying oscillation. In Eq. (2), the vibration amplitude A_n at time nT (T – period duration) and A_{n+k} – the vibration amplitude k oscillation periods later at time $(n+k)T$ are shown, where n and k are whole numbers. To obtain the current damping behaviour of a damped system, two consecutive oscillation amplitudes are therefore considered [33] (Fig. 4).

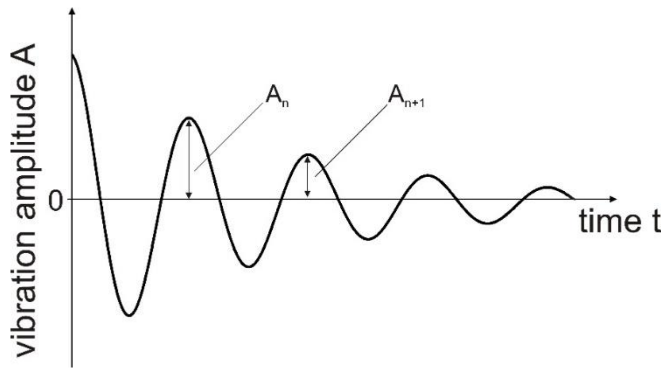

Fig. 4 – Idealised behaviour of a decaying vibration of a bending sample clamped at one side.

Based on Eq. (1), the oscillation amplitude A corresponds to the maximum displacement z', so that the logarithmic decrement δ can be measured as a function of the strain amplitude ε_{max}.

Fig. 5 shows the experimental setup for determining material damping. It consists of a hollow metallic substructure, weighted with sand on the inside. A high mass is necessary to reduce any apparatus vibrations and shift their frequencies to a lower range (→ according to the natural frequency of a spring pendulum: $\omega = \sqrt{D/m}$, where ω – circular frequency, D – spring constant, m – mass). This prevents any interference with the sample vibration. Additionally, each screw connection is insulated with rubber mats to restrict the transmission of parasitic vibrations to the sample body.

A metallic cylinder is rotated using a hand crank. On this cylinder, there is a bevelled cuboid that touches the free end of the bending sample and sets it into vibration. Depending on the degree of overlap between the bevelled cuboid and the free end of the bending beam, a change in the starting amplitude can be achieved. When there is no longer contact with the sample, the deflected bending beam can freely oscillate.

The oscillation is measured using a laser triangulation sensor (model: ILD1320-100, Micro-Epsilon, Ortenburg, Germany) with a set sampling rate of 2000 measurement points per second. It is attached above the free end of the sample and records the vibration data as a function of time by measuring distance data. The software of the laser transfers the data to a PC and visualises it.

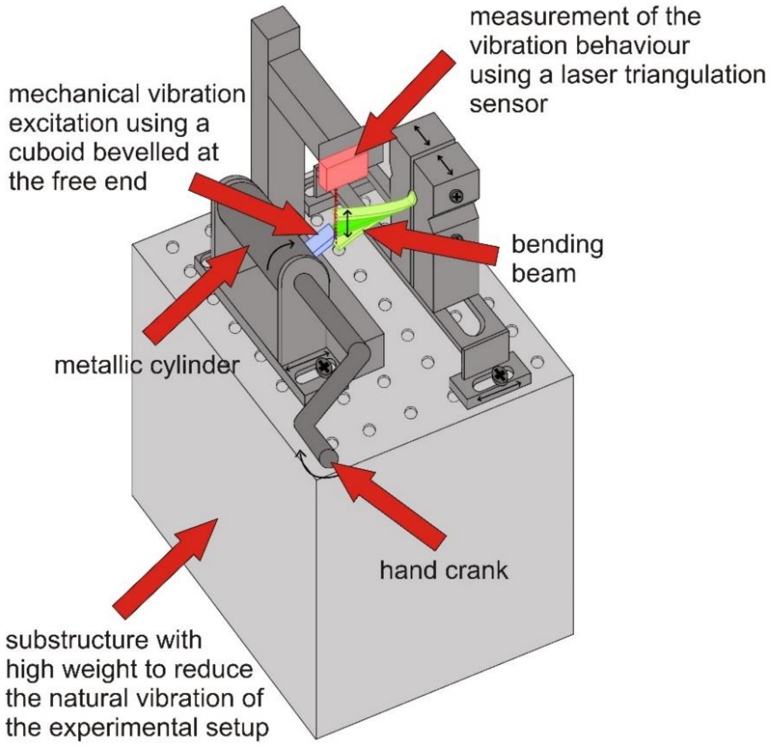

Fig. 5 – Experimental damping setup. Adopted from Ref. [30] (modified).

In Fig. 6, the decaying signal of the excited sample vibrating is shown as a function of time. In the resting state, the laser triangulation sensor is located at a distance of approximately 42 mm from the sample surface of the free end of the sample (offset). To calculate the logarithmic decrement, only vibration amplitudes around the zero position are allowed (see Fig. 4). For this reason, the raw data are adjusted by this offset.

As can be seen from Fig. 6, the sample is deflected towards the laser triangulation sensor. To determine the logarithmic decrement, the lower portion of the decaying curve is used here. In order to avoid the influence of Coulomb friction, the highest amplitude resulting from contact of the bevelled cuboid with the free end of the sample is disregarded, and only the second amplitude (related to the lower portion of the decaying curve) is used for calculating the logarithmic decrement δ.

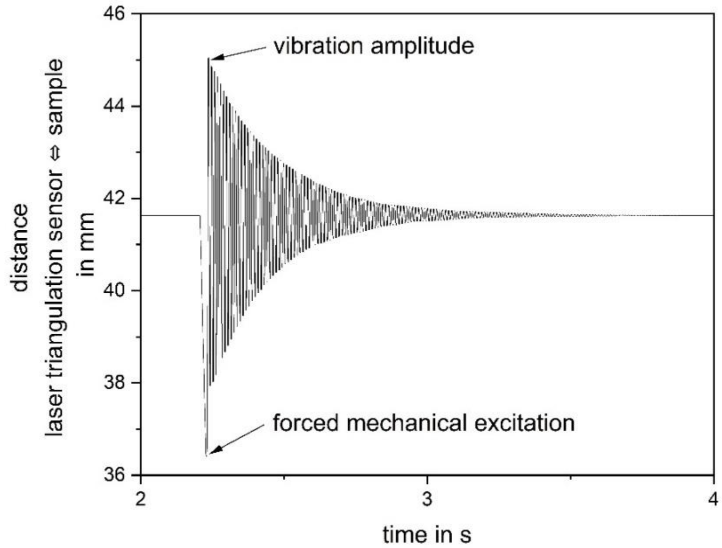

Fig. 6 – Decaying vibration of a bending sample clamped at one side using the experimental damping setup.

As already mentioned, for the calculation of the (strain-dependent) logarithmic decrement, two consecutive vibration amplitudes are used, however, according to Eq. (1), where z' corresponds to the vibration amplitude, only one amplitude is used for the calculation of ε_{max} of the sample at the clamping location. Since neither the higher amplitude nor the lower amplitude sufficiently represents the actual ε_{max}, a weighted average of two consecutive amplitudes is determined in this work for the calculation of ε_{max}.

Determination of the bending modulus. Knowledge of the specific density of the samples was required to calculate the bending modulus (being the ratio of stress to strain during a flexural deformation and quantifying a material's stiffness). The bending modulus is similar to the respective tensile modulus. However, in anisotropic materials like wood the flexural stress is generally higher than the tensile stress [34] leading to a slightly higher bending modulus under bending load.

Since the microstructure within the tree varies and only the specification of a data range is useful for biological materials, no mechanical properties should be taken from literature if it is possible to determine the relevant data for the experiment itself. Following this fact, the specific density of each bending beam used was measured based on the Archimedes' principle. Firstly, the weight of the sample in air was determined, and then in water (condition: 20°C, 1013.25 hPa air pressure). From the difference in the weight forces obtained, the buoyancy force on the sample can be determined, from which the density of the bending beam can ultimately be calculated. This method is employed when test samples do not conform to common shapes (such as spheres, cubes, etc.).

The Archimedes' principle is generally known and will not be further discussed at this point. However, it is worth noting that this experimental procedure is not easily applicable to porous materials like wood, due to wood's hygroscopic nature. This means that the lumens or pores of the wood fill with water, potentially leading to inaccurate density determinations. For this reason, the samples were placed in a vacuum bag and sealed using a vacuum sealer device (Fresko®, model: V5, 120 W, Bonsen Electronics Limited, Guangdong, China). This prevents water from penetrating the wood. The vacuum bag, with its contents, ultimately constitutes a composite. The specific density of the wood was determined by calculating the respective volume fraction of the composite components (using 'rule of mixtures', *e.g.* Ref. [35]). These components were: the vacuum bag, the threads used for suspension, an attached load (→ ensures that the composite is fully immersed in water), and the wood sample. Since the power of the vacuum sealer device was relatively low, it was assumed that the air in the lumens remains mostly intact, allowing for a more realistic value of the specific density of the used wood sample to be obtained.

As the bending sample shows approximately harmonic decay behaviour immediately after vibration excitation, the vibration frequency f can be calculated according to $f = 1/T$ (T – time of oscillation). Knowing f and the specific density ρ, obtained from the mentioned density measurement based on the Archimedes' principle, the bending modulus E_{bend} (here in the unit N/mm^2 (or MPa)), can be determined as [36]

$$E_{bend} = 10^{-12} 4\pi^2 f^2 \frac{l^4}{c^4} \frac{\rho ab}{I_y}, \tag{3}$$

where c is a constant (eigenvalue) taken from the modal analysis of a cantilever beam. Using c = 1.875 the first vibration mode of such a beam is described. I_y is the area moment of inertia of a rectangle (→ end face of the bending beam) with respect to the resistance to bending around the Y-axis, with $I_y = \frac{a^3 b}{12}$. The used sample dimensions (a, b, l) and coordinate system (necessary to determine I_y) refer to the information in Fig. 3.

Determination of the apparatus damping. Damping is subject to the superposition principle, meaning that various external damping mechanisms (such as apparatus damping) can overlap and thus distort material damping. It is not easy to detect this additional damping, and in individual cases it may be difficult to determine. This makes it challenging to compare absolute damping values. Relative changes between damping data naturally remain even if the apparatus damping is retained.

In the following, the apparatus damping δ_a – which can be classified as a systematic error and should be as small as possible – of the experimental setup was estimated. For this purpose, an extremely stiff reference sample (reference material: austenitic titanium-stabilised stainless steel X6CrNiMoTi17.12.2; modulus of elasticity E = 186000 N/mm^2 at 20°C [37]) was used, which was subjected to a maximum strain amplitude of approximately 0.8 (in terms of $\varepsilon_{max} \times 1000$). Due to the high stiffness of the sample, the vibration energy was transferred to the apparatus which was noticeable when touching the experimental setup. Therefore, the temporal decay of the sample vibration also included the damping behaviour of the apparatus.

As shown in Fig. 7, the logarithmic decrement δ is plotted against the logarithm of the maximum strain amplitude ε_{max}. In the range of small strain amplitudes, there is a parallelism to the X-axis, while for higher strain amplitudes, an extremely steep increase in damping is observed. In the case of small strain amplitudes, the damping did not decrease to zero due to residual vibrations induced by the equipment, which was interpreted as apparatus damping with a value of approximately $\delta_a \approx 10^{-5}$. The measured damping data of wood were adjusted by subtracting δ_a to remove this damping offset.

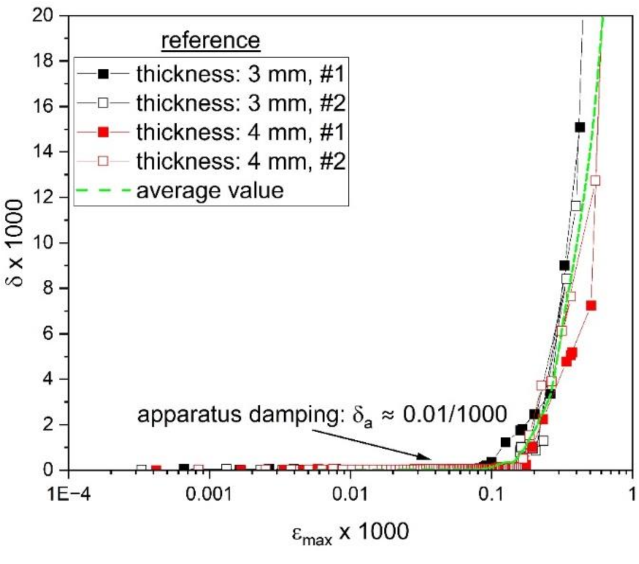

Fig. 7 – Strain-dependent damping of the reference material for determining the apparatus damping δ_a.

Determination of the air damping. In addition to apparatus damping, material damping is also influenced by the air resistance (air damping). This kind of damping must be considered and subtracted from the damping data of wood. As the apparatus does not allow measurements under vacuum conditions, the magnitude of the air damping has to be estimated.

For this purpose, a sample with a low specific density (measured value based on the Archimedes' principle: ρ = 1012 kg/m^3) was produced using a 3D printer. ABS (Acrylonitrile Butadiene Styrene) filament was applied for the 3D printing process of samples which were used for testing the experimental damping setup with regard to the reproducibility of data. ABS is a thermoplastic polymer and especially known for its high impact resistance at low temperatures [38]. According to the literature, it has a specific density of 1050 kg/m^3 [39]. As 3D-printed objects always have empty spaces [40], the measured specific density of the samples is therefore lower than the specific density of the filament listed in the literature. Such printed samples are relatively easy to produce and can be subjected to higher bending forces without breaking.

In Fig. 8, the strain-dependent damping of an ABS bending beam is shown. A total of six measurements were conducted. The resonance frequency was about 95 Hz, and a bending modulus E_{bend} of approximately 1842 N/mm^2 was determined using Eq. (3). This value of the bending modulus is consistent with data from the literature obtained from tensile tests [41]. The authors of these tests point out the directionality of the measurements, which leads to different values for the modulus of elasticity. Accordingly, a range for the elasticity modulus from 1800–2200 N/mm^2 was obtained [41]. The calculated bending modulus lies within this range. Furthermore, from the six measurements in Fig. 8, it can be observed that reproducible results can be obtained with the measuring apparatus.

The air damping was determined using ABS samples which were fitted with an adapter at the free end (Fig. 9). This adapter which was also produced by 3D printing using ABS filament gave the vibrating ABS sample wings to increase the air resistance.

Such an adapter increases the mass of the bending beam, which leads to a reduction in its natural frequency f. A calculation carried out for this purpose resulted in a reduction of f of approximately 35%. Thermoelastic damping by transverse heat flow from the compressed to the extended surface of the bending beam could cause damping that is sensitive to the frequency of vibration [42]. However, more dominant material-specific damping mechanisms exist, especially in polymers which behave viscoelastically. Polymer damping is due to moving main molecular chains or side-groups of them [43]. The damping properties resulting from the viscoelasticity depend on material type, its structure, excitation frequency, temperature, relative humidity etc. [44].

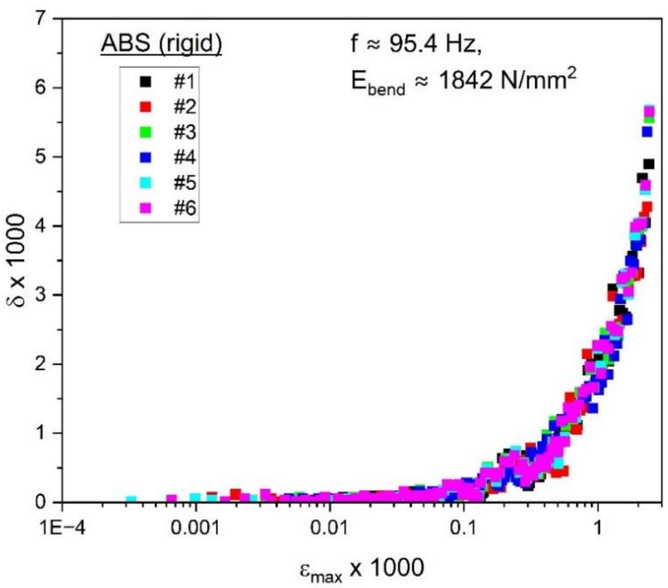

Fig. 8 – Testing the reproducibility of the damping measurements using 3D-printed bending samples produced with ABS filament.

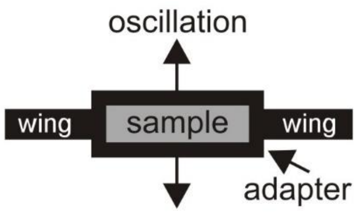

Fig. 9 – An adapter equipped with wings at the free end of the oscillating bending beam.

To illustrate the influence of air damping, the simple harmonic motion with oscillation amplitude A should be used whose frequency f and velocity v of a surface particle are linked by the following equation (*e.g.* Ref. [45]):

$$v_{max} = 2\pi f A. \quad (4)$$

F_{air} is the air resistance (force of resistance) of an object (here, the bending beam) moving in air with

$$F_{air} = \frac{1}{2}\rho_{air} c_x S_{eff} v^2 \,, \quad (5)$$

where ρ_{air} the specific density of air, c_x is the air resistance coefficient (drag coefficient or coefficient of influence of the body shape on air resistance) and S_{eff} the effective area facing the air [46].

Power P and force F of a mechanical system are connected to each other through the relationship $P = Fv$. Therefore, the power necessary to overcome the air resistance, *i.e.* power loss due to air damping, P_{air}, is writable as

$$P_{air} = \frac{1}{2}\rho_{air}c_x S_{eff} v^3. \tag{6}$$

Combining Eq. (4) and Eq. (6) leads to

$$P_{air,max} = 4\pi^3 \rho_{air} c_x S_{eff} A^3 f^3. \tag{7}$$

Under the same measurement conditions, A and the oscillation frequency f are the decisive measured variables that lead to a loss of power in the oscillation. Therefore, the following applies:

$$P_{air,max} \sim A^3 f^3. \tag{8}$$

Although this estimate is approximate, it shows that a treatment of air damping is justified. Equation (8) suggests that the loss due to air damping increases significantly with increasing vibration frequency and vibration amplitude. However, it diminishes considerably as the amplitude decreases, assuming the vibration frequency remains roughly constant, typical in damped systems. For this reason, air damping must be taken into consideration, particularly for high vibration amplitudes, and is almost negligible for low vibration amplitudes.

To measure the influence of air damping, the sample chamber of the apparatus would be gradually evacuated, thereby reducing the air pressure and, thus, the power loss due to air damping. This would lead to an increase in the oscillation frequency. However, since achieving vacuum conditions is not feasible in the current experimental setup, using wings (as shown in Fig. 9), which introduce increased air resistance, is expected to cause a decrease in frequency as the wing area is increased. Therefore, the approach taken is opposite: employing a successive reduction of the wing area in the experiment suggests a transition from higher air damping (→ the influence of air damping would become apparent when compared with damping measurements under vacuum conditions) to lower air damping. Such a procedure allows for an estimation of the influence of air damping, which, as per Eq. (8), is expected to decrease as oscillation amplitudes decrease. This can be observed in Fig. 10. At lower vibration amplitudes (area B), which means low ε_{max}, a maximum influence on the damping of approximately 10% can be assumed in the range of ε_{max} used in this work.

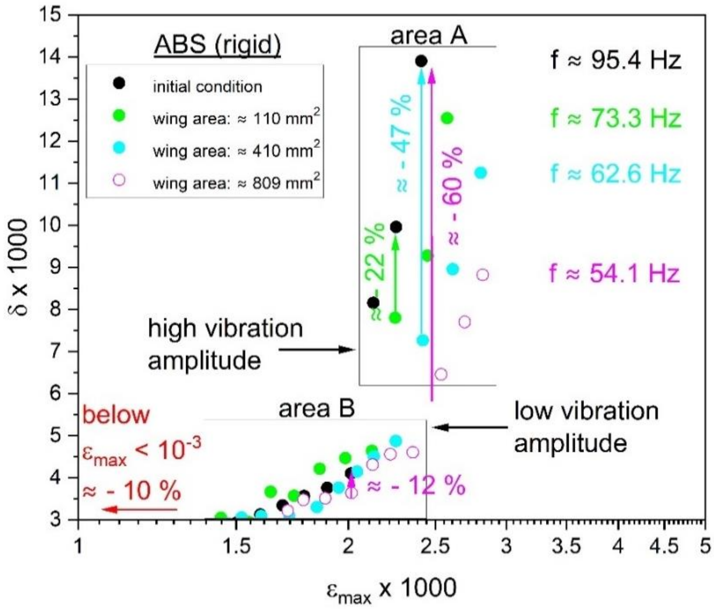

Fig. 10 – Influence of air damping using wings.

3. RESULTS

In Fig. 11, the strain-dependent damping of Kiri wood from Georgia can be seen. The bending modulus E_{bend} was calculated according to Eq. (3) and added as well.

The damping curves can be divided into a strain-independent range (δ_0 → parallel to the X-axis) and a strain-dependent range ($\delta_h(\varepsilon_{max})$ → increase with increasing strain) where δ_h is the hysteretic damping. Such behaviour is well known for strain-dependent damping measurements of metals [47]. A noticeable increase in material damping is observed at a strain amplitude of approximately 0.1 (in terms of $\varepsilon_{max} \times 1000$). The tangential fibre orientation T appears to result in a higher material damping at the same strain amplitude.

Kiri wood from Germany (Fig. 12) shows the same curve progression as Kiri wood from Georgia. Here, TR and Tr are the directions that lead to increased damping. The curve profile, represented by the averaged curve, is similar to the profile of the averaged curve of Georgian wood. The bending modulus is higher in the Kiri wood sample from Germany compared to the Georgian wood, which results in slightly higher strength.

A significant difference in both the strain-dependent damping and the bending modulus can be observed in the Italian Kiri wood samples (Fig. 13). The bending modulus is significantly lower than that of the Georgian or German samples. For example, when considering the logarithmic decrement at maximum strain amplitude with a value of 1 (in terms of $\varepsilon_{max} \times 1000$), an approximately 30% lower value of material damping is recorded. The maximum damping is only reached at higher strain amplitudes. The wood tested is less rigid than the samples from Georgia and Germany.

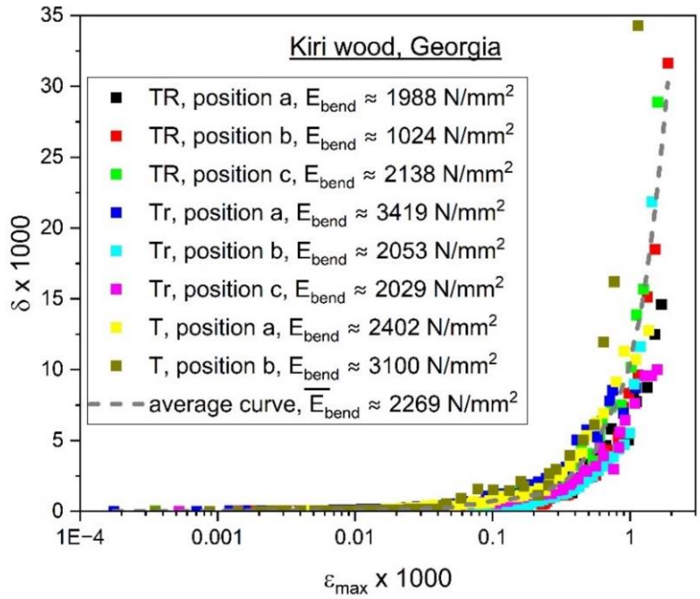

Fig. 11 – Strain-dependent damping of Kiri wood from Georgia in consideration of the fibre orientation. The calculated bending modulus E_{bend} is added.

Fig. 14 – Fig. 16 show the results of strain-dependent damping measurements of Kiri wood samples from Spain. There was mainly a radial fiber orientation present. In all cases, the bending modulus is greater than the value of the samples from Italy, Germany, and Georgia. In the higher strain range, a comparatively high damping is revealed.

Fig. 17 shows the respective averaged strain-dependent damping curves. It becomes clear once again that the damping of the Kiri wood samples from Georgia and Germany are very similar. To illustrate the difference in damping data, the data was taken at maximum strain amplitudes of 0.1 and 1 (in terms of $\varepsilon_{max} \times 1000$, see also reference lines) and are shown in Table 3. It is evident that the samples from Spain have approximately double the values of strain-independent damping compared to the other samples. In the strain-dependent damping range, the samples from Italy exhibit lower damping than the samples from Georgia and Germany. However, the damping values of the samples from Spain at this strain amplitude is approximately double that of the others.

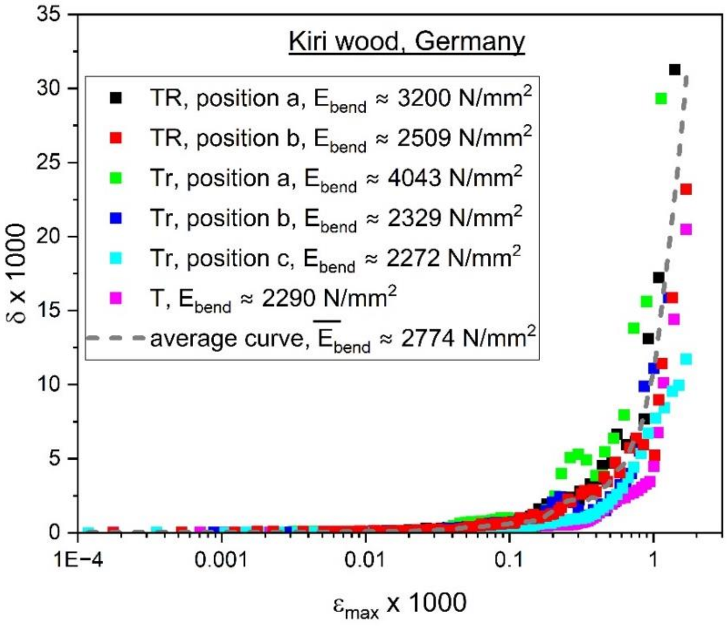

Fig. 12 – Strain-dependent damping of Kiri wood from Germany in consideration of the fibre orientation. The calculated bending modulus E_{bend} is added.

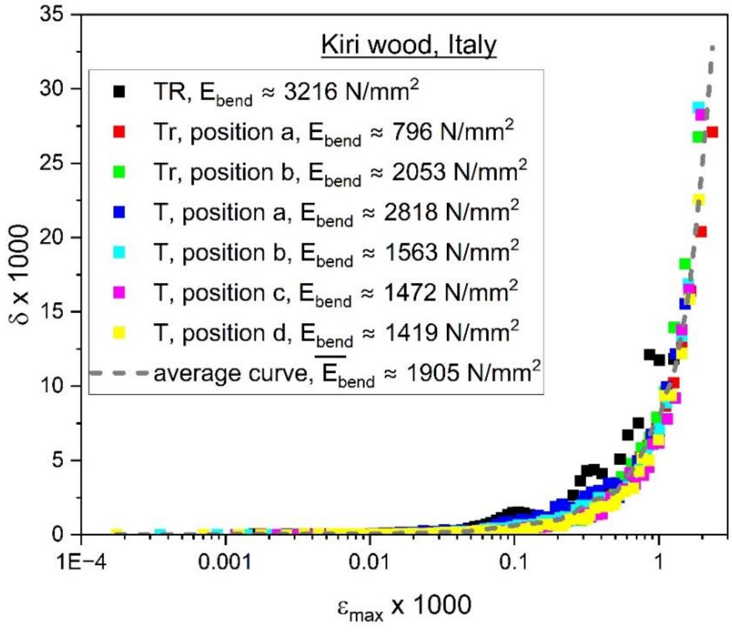

Fig. 13 – Strain-dependent damping of Kiri wood from Italy in consideration of the fibre orientation. The calculated bending modulus E_{bend} is added.

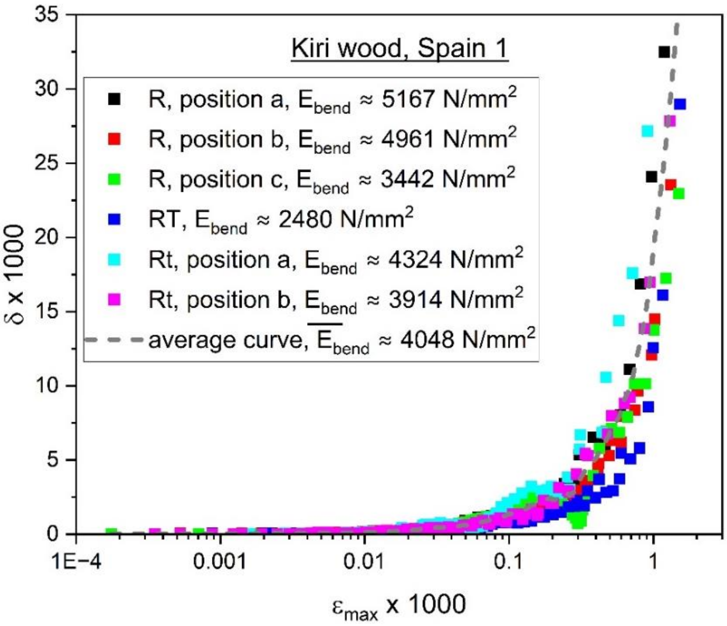

Fig. 14 – Strain-dependent damping of Kiri wood from Spain (1) in consideration of the fibre orientation. The calculated bending modulus E_{bend} is added.

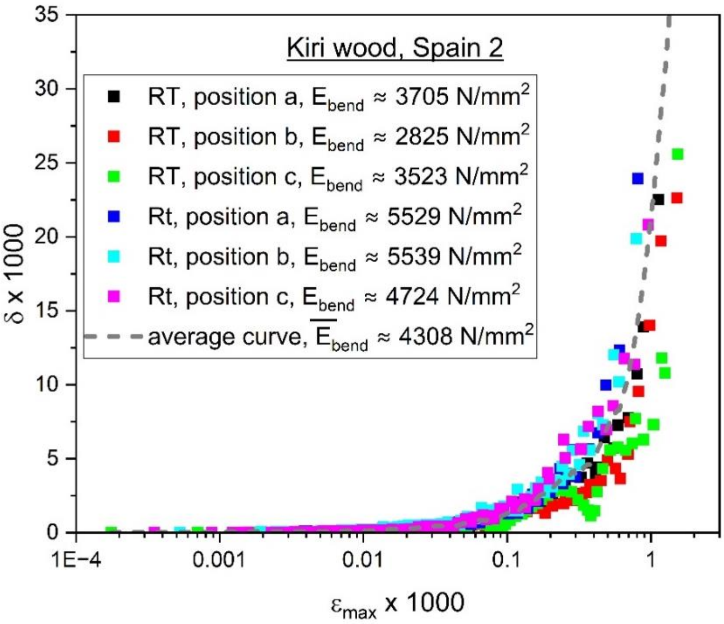

Fig. 15 – Strain-dependent damping of Kiri wood from Spain (2) in consideration of the fibre orientation. The calculated bending modulus E_{bend} is added.

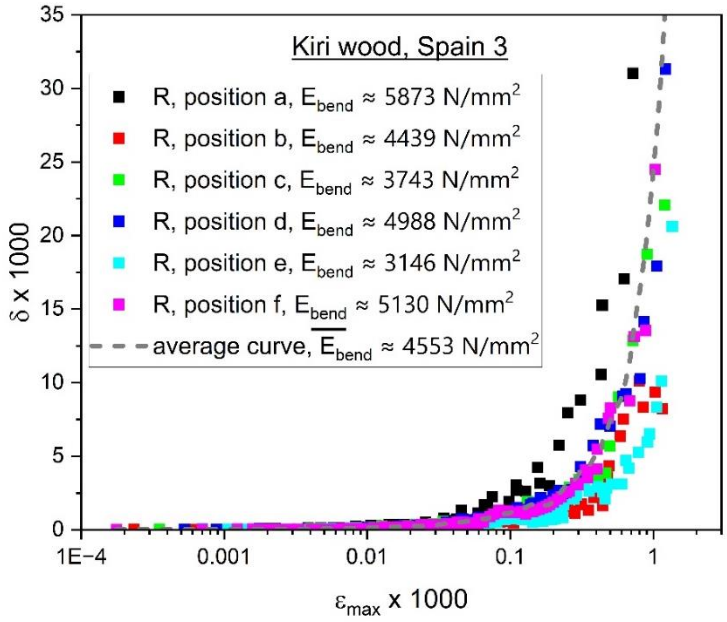

Fig. 16 – Strain-dependent damping of Kiri wood from Spain (3) in consideration of the fibre orientation. The calculated bending modulus E_{bend} is added.

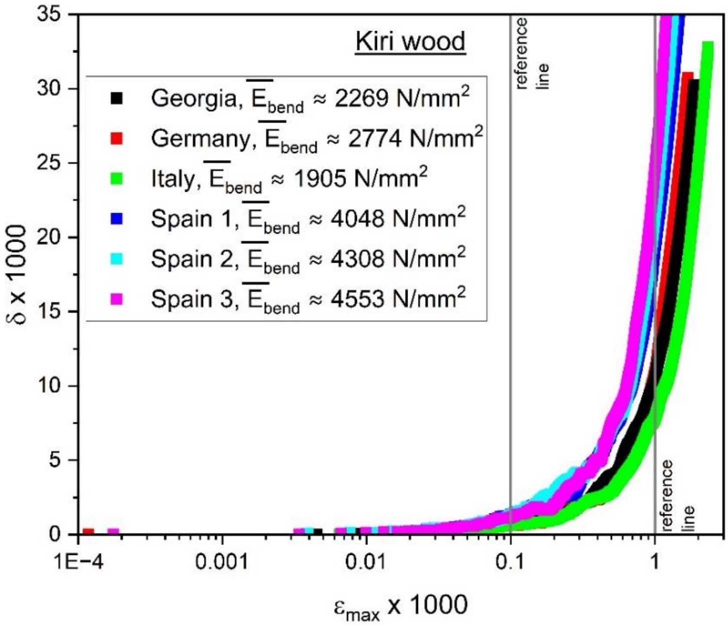

Fig. 17 – Mean strain-dependent damping curves of Kiri wood. The calculated mean bending modulus $\bar{E}_{bend}$ is added.

Table 3

Comparison of damping data at different strain amplitudes

$\varepsilon_{max} \times 1000$	ε_{max} in %	$\delta \times 1000$, Georgia	$\delta \times 1000$, Germany	$\delta \times 1000$, Italy	$\delta \times 1000$, Spain 1	$\delta \times 1000$, Spain 2	$\delta \times 1000$, Spain 3
0.1	0.01	0.74	0.61	0.63	1.36	1.33	1.16
1	0.1	10.52	10.92	7.83	19.19	21.41	24.46

4. DISCUSSION

According to Golovin [48], a damping categorisation can be made on the basis of the damping value at ε_{max} about 0.1 (in %, see Table 3). Based on this classification, Kiri wood can be regarded as a medium damping material.

It is not meaningful to publish exact damping data but to provide a range. The fibre direction plays a major role [49], and the deviation of damping data even within wood from the same tree is different. It is an organic material with local microstructural peculiarities. Because of this, only approximate values for certain properties can be given. Without specifying a strain, even such damping values are technically irrelevant.

It is necessary to classify the results of the strain-dependent damping of Kiri wood. In this context, the results of the non-invasive German variant of Kiri wood are used and compared to the strain-dependent damping of the softwood pine and the hardwood beech. This comparison is shown in Fig. 18.

It is obvious that the bending modulus of beech wood and pine wood depends on the fibre direction and ranges from approximately 9000 N/mm^2 to 13800 N/mm^2 for beech wood (literature value for American beech: 11900 N/mm^2 [49]) and between 9000 N/mm^2 and 12500 N/mm^2 for pine wood (literature value: 8500 N/mm^2 – 13700 N/mm^2 [49]).

Kiri wood has an average bending modulus of around 3200 N/mm^2 and is therefore to be described as soft. According to literature, its bending modulus ranges from 2651 N/mm^2 to 4917 N/mm^2 [9]. Both beech wood and pine wood are used as tonewoods. The damping behaviour of Kiri wood is very similar to that of beech wood. So, it is not surprising that Kiri wood is used as tonewood, too. The damping potential can be used in areas where higher sound absorption is required. However, Jang and Kang [50] reported that among the three species Binuang, Balsa and Paulownia, the Paulownia wood showed the lowest sound absorption coefficient. Gas permeability, pore size and through-pore porosity decreased due to the effect of tyloses in the vessels which makes it difficult to absorb sound.

In instrument making, the emission of energy is important. Excessive variation in energy emission due to strong frequency dependence of the damping of the construction material should therefore be avoided. Looking at the sound absorption coefficient as a function of frequency (frequency range: 250 Hz to 6400 Hz), it becomes clear that Paulownia wood has a comparatively constant value [50]. Spruce wood is considered established tonewood that is used in instrument construction [51]. Own measurements showed a frequency-dependent damping of old and new spruce wood at a moisture content of nearly 8% (frequency range: 0.3 Hz to about 70 Hz) [52]. In measurements by Rohloff [53], a frequency-independent damping of spruce wood in a frequency range of 10 Hz to 2000 Hz was even found. Such behaviour also applies to Paulownia wood despite its low (but constant) sound absorption coefficient. The wood acoustically behaves consistently over a wide frequency range and is therefore universally usable. Since wood is a renewable resource, particularly with Paulownia wood, the properties of sustainability, aesthetics, and functionality are combined. The wood is also very light, thus, less energy is used in transporting this material.

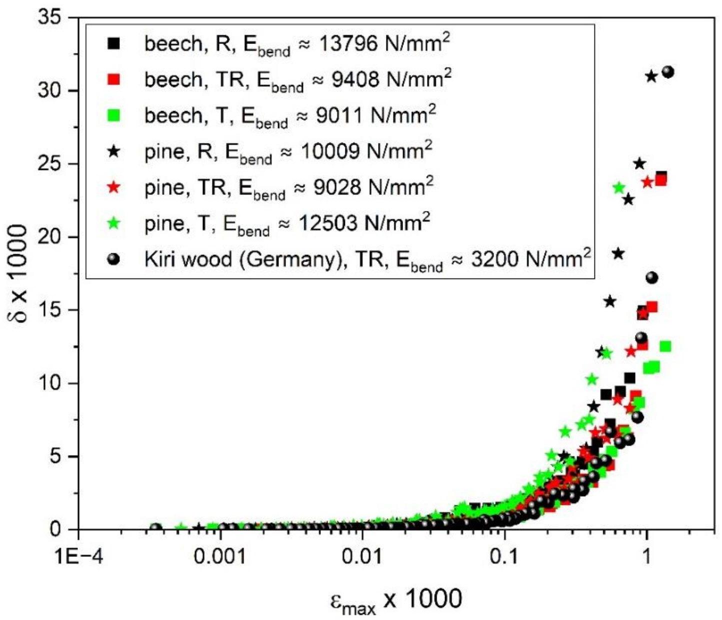

Fig. 18 – Strain-dependent damping of different woods. The calculated bending modulus E_{bend} is added.

As can be seen in Fig. 11 – Fig. 16 all damping curves have the same shape, which indicates a similar damping mechanism. In metals, the strain amplitude dependency of the loss tangent is known from an unpinning process from obstacles (*e.g.* impurity atoms or small precipitates) as explained in the Granato-Lücke theory of dislocation damping [54]. Following this approach, a similar mechanism is assumed here whereas the obstacles is a cluster consisting of connection of biopolymer segments with water molecules. For small strain amplitudes, it is presumed that only molecular segments exert a small movement (bowing out mechanism). At higher strain amplitudes, the actual bonding force between the water molecules and some molecule segments is no longer sufficient and they begin to assume a new potential minimum and bond with new water molecules. This process increases with rising strain amplitude. The mentioned approach is based on studies of Becker and Noack [55]. They point out that groups of molecules from parts of cellulose, hemicellulose and lignin (structural components of the wood cell wall) can move. Furthermore, there is an influence of water molecules which are connected with these groups of molecules by sorption forces and which produce variations in the distance between molecules, of the mobility and the state of orientation of the molecules as well as of the dipole moment of polar groups. In the wood fibre system, the potential adsorption sites are the hydroxyl groups and the carboxyl groups [56]. Amorphous wood polymers or segments have a higher affinity to form a bond with water [57]. Therefore, the moisture content has a significant influence on the wood damping. This was shown in a former own work [31].

5. CONCLUSIONS

Effective plantation cultivation is essential to meet the global existential threat from climate change and environmental degradation. An innovative agricultural management capable of facing the current environmental challenges is needed. A fast-growing timber which demonstrably enables plantation cultivation is Paulownia wood which is also known as Kiri wood.

The usual varieties are considered invasive, but a new variety is not. This non-invasive Paulownia variety is called Paulownia NordMax21® and is a German hybrid of Paulownia tomentosa and Paulownia fortunei. Its damping behaviour was investigated and compared with common Paulowina varieties harvested in Georgia, Italy and Spain.

One important mechanical property of wood is its material damping because it contributes to the sound characteristics. The damping was measured as logarithmic decrement of freely decaying bending vibrations and determined as a function of the maximum strain amplitude. An experimental damping setup was built up. In order to measure the material damping as accurately as possible, the apparatus damping and the damping due to air friction were determined and subtracted from the measurement data of the samples.

All damping curves could be divided into a strain-independent and a strain-dependent range where the latter one is interpreted as hysteretic damping. Such behaviour is well known for strain-dependent damping measurements of metals where pinning/unpinning of defects from pinning points in the structure (*e.g.* dislocations) can be found (Granato-Lücke model). Basically, the same approach was proposed here to explain the strain-dependent damping measurement curves. The measurements showed that Paulownia wood can be considered as a medium damping material.

In this study chain molecules are assumed to play the similar role as dislocations in metals. The water inside the wood interacts with molecular segments being part of cell wall. This interaction leads to variations in the distance between these segments, to a change of the mobility as well as the state of orientation of the molecules.

Due to the complexity within the wood structure, results on damping properties are always associated with a certain degree of uncertainty because the growing conditions at the tree's location play an important role and significantly determine the mechanical properties. This was evident in the determination of the bending modulus, too.

Acknowledgements. Prof. dr. Jürgen Göken would like to thank the KIRITEC GmbH (Tönisvorst, Germany) for providing the Kiri wood used in this work. The Meyer Möbelmanufaktur GmbH (Westoverledingen, Germany) is thanked for producing the Kiri wood samples. Special thanks go to the students Ms. A. Liehm and Mr. K. Legene, who carried out the recording of the raw data as part of their respective bachelor thesis.

REFERENCES

1. https://www.fao.org/3/X1674E/X1674E05.htm (access on 22nd January 2024).
2. https://www.globaltimber.org.uk/rwevolume.htm (access on 22nd January 2024).
3. Food and Agriculture Organisation of the United Nations (FAO), "Global Forest Sector Outlook 2050 – Assessing Future Demand and Sources of Timber for a Sustainable Economy." Background paper for The State of the World's Forests 2022. FAO Forestry Working Paper, No. 31. Rome, page 9. https://doi.org/10.4060/cc2265en.
4. https://commission.europa.eu/strategy-and-policy/priorities-2019-2024/european-green-deal_en (access on 22nd January 2024).
5. V. Rolo, *Agroforestry for Sustainable Food Production*, In: V. Rolo (ed.), Agroforestry and Sustainable Agricultural Production. MDPI, Basel, Switzerland, 2022, p. 1.
6. M. Báder, R. Németh, Á. Vörös, Z. Tóth, A. Novotni, *The Effect of Agroforestry Farming on Wood Quality and Timber Industry and its Supportation by Horizon 2020*, Agroforest Syst. **97**, 587-603 (2023). https://doi.org/10.1007/s10457-023-00812-8.
7. United Nations and the Food and Agriculture Organisation of the United Nations, *Circularity Concepts in Wood Construction*. ECE/TIM/DP/95 (2023). ISBN: 978-92-1-117328-4.
8. P. Icka, R. Damo, E. Icka, *Paulownia Tomentosa, a Fast Growing Timber*, The Annals of "Valahia" University of Targoviste, 2016. DOI: 10.1515/agr-2016-0003.
9. M. Jakubowski, *Cultivation Potential and Uses of Paulownia Wood: A Review*, Forests **13**, 668 (2022). https://doi.org/10.3390/f13050668.
10. V.B. Woods, *Paulownia as a Novel Biomass Crop for Northern Ireland? – A Review of Current Knowledg*e. Agri-Food Biosciences Institute (AFBI), Hillsborough, Northern Ireland (2008).
11. https://www.eea.europa.eu/articles/forests-health-and-climate-change/key-facts/trees-help-tackle-climate-change (access on 23th January 2024).
12. O. Dubova, O. Voitovych, O. Boika, *Paulownia Tomentosa – New Species for the Industrial Landscaping*. Curr. Trends Nat. Sci. **8** (16), 19-24 (2019).
13. https://paulownia.pro (access on 21st January 2024)
14. P.D. Erskine, D. Lamb, G. Borschmann, *Growth Performance and Management of a Mixed Rainforest Tree Plantation*, New For. **29**, 117-134 (2005). https://doi.org/10.1007/s11056-005-0250-z.
15. R. Williams, H. Wang, *Effects of Wildfire and the Presence of the Invasive Paulownia tomentosa on the Regeneration of Native Tree Species in North-Central Appalachia*, Fire **4**, 60 (2021). https://doi.org/10.3390/fire4030060.

16. https://www.paulownia.at/product/nordmax-21 (access on 25th January 2024).
17. https://www.kiritec.eu (access on 18th January 2024).
18. https://wegrow-croptec.com/en/how-to-grow-2/kiri-wood (access on 18th January 2024).
19. C. Mai, U. Schmitt, P. Niemz, *A Brief Overview on the Development of Wood Research*, Holzforschung **76** (2), 102-119 (2022). https://doi.org/10.1515/hf-2021-0155.
20. K. Kránitz, W. Sonderegger, C.-T. Bues, P. Niemz, *Effects of Aging on Wood: A Literature Review*, Wood Sci. Technol. **50**, 7-22 (2016). https://doi.org/10.1007/s00226-015-0766-0.
21. N. Labonnote, *Damping in Timber Structures*, PhD thesis, Faculty of Engineering Science and Technology, Department of Structural Engineering, Norwegian University of Science and Technology, Trondheim, Norway, 2012.
22. J.I. Dunlop, *Damping Loss in Wood at Mid Kilohertz Frequencies*, Wood Sci. Technol. **12** (1), 49-62 (1978). https://doi.org/10.1007/BF00390010.
23. M.S. Blanter, I.S. Golovin, H. Neuhäuser, H.-R. Sinning, *Internal Friction in Metallic Materials – A Handbook*, Springer, Berlin, Germany, 2007, p. 3.
24. R. Lakes, Viscoelastic Materials (ch. 1), Cambridge University Press, Cambridge, United Kingdom, 2009.
25. F. Orban, *Damping of Materials and Members in Structures*, J. Phys.: Conf. Ser. **268**, 012022 (2011). DOI: 10.1088/1742-6596/268/1/012022.
26. I. Brémaud, *Acoustical Properties of Wood in String Instruments Soundboards and Tuned Idiophones: Biological and Cultural Diversity*, J. Acoust. Soc. Am. **131** (1), 807-818 (2012). https://doi.org/10.1121/1.3651233.
27. T. Ray, J. Kaljun, A. Straže, *Comparison of the Vibration Damping of the Wood Species Used for the Body of an Electric Guitar on the Vibration Response of Open-Strings*, Materials **14** (18), 5281 (2021). https://doi.org/10.3390/ma14185281.
28. U.G.K. Wegst, *Wood for Sound*, Am. J. Bot. **93** (10), 1439-1448 (2006). https://doi.org/10.3732/ajb.93.10.1439.
29. M. Jakob, A.R. Mahendran, W. Gindl-Altmutter, P. Bliem, J. Konnerth, U. Müller, S. Veigel, *The Strength and Stiffness of Oriented Wood and Cellulose-fibre Materials: A Review*, Prog. Mater. Sci. **125**, 100916 (2022). https://doi.org/10.1016/j.pmatsci.2021.100916.
30. A. Liehm, *Messungen der dehnungsabhängigen Dämpfung von Paulownia-Holz (Measurements of the Strain-dependent Damping of Paulownia Wood)*, Bachelor Thesis, Faculty of Maritime Sciences, Laboratory of Materials Physics, University of Applied Sciences Emden/Leer, Leer, Germany, 2024.
31. J. Göken, N. Saba, I.S. Golovin, *Damping of Spruce Wood at Different Strain Amplitudes, Tempertures and Moisture Contents*, Rom. J. Phys. **68**, 903 (2023).
32. Z. Trojanová, P. Palček, P. Lukáč, M. Chalupová, *Internal Friction in Magnesium Alloys and Magnesium Alloys-Based Composites*, (ch. 2), In: M. Aliofkhazraei (ed.), Magnesium Alloys. IntechOpen Limited, London, United Kingdom, 2017. DOI: 10.5772/67028.
33. M.S. Blanter, I.S. Golovin, H. Neuhäuser, H.-R. Sinning, *Internal Friction in Metallic Materials – A Handbook*, Springer, Berlin (2007), p. 10.
34. E. Alfredo Campo, *Mechanical Properties of Polymeric Materials*, In: E. Alfredo Campo (ed.), *Selection of Polymeric Materials: How to Select Design Properties from Different Standards*, William Andrew Publishing, Norwich, New York, USA (2008), pages 41-101. https://doi.org/10.1016/B978-081551551-7.50004-8.
35. M.F. Ashby, *Selecting the Components of Composites*, J. Phys. IV **3** (C7) 1595-1600 (1993). https://doi.org/10.1051/jp4:19937250.
36. S. Sohn, *Feasibility Study on the Use of Wireless Accelerometers in the Experimental Modal Testing*, J. Supercomput. **72**, 2848-2859 (2016). https://doi.org/10.1007/s11227-016-1628-8.
37. J. Brnic, G. Turkalj, M. Canadija, D. Lanc, *AISI 316Ti (1.4571) Steel - Mechanical, Creep and Fracture Properties Versus Temperature*, J. Constr. Steel Res. **67** (12), 1948-1952 (2011). https://doi.org/10.1016/j.jcsr.2011.06.011.
38. https://www.3dnatives.com (access on 6th February 2024).

39. A.P. Agrawal, V. Kumar, J. Kumar, P. Paramasivam, S. Dhanasekaran, L. Prasad, *An Investigation of Combined Effect of Infill Pattern, Density, and Layer Thickness on Mechanical Properties of 3D Printed ABS by Fused Filament Fabrication*, Heliyon **9 (6)**, e16531 (2023). https://doi.org/10.1016/j.heliyon.2023.e16531.
40. J. Göken, N. Saba, *Damping Behaviour Analysis of 3D Printed Samples with Pores*, Acta Phys. Pol. A **138** (6), 844-853 (2020). DOI: 10.12693/APhysPolA.138.844.
41. T. Vukasovic, J.F. Vivanco, D. Celentano, C. García-Herrera, *Characterization of the Mechanical Response of Thermoplastic Parts Fabricated with 3D Printing*, Int. J. Adv. Manuf. Technol. **104**, 4207-4218 (2019). https://doi.org/10.1007/s00170-019-04194-z.
42. J. Göken, W. Riehemann, *Thermoelastic Damping of the Low Density Metals AZ91 and DISPAL*, Mater. Sci. Eng. A **324** (1-2), 134-140 (2002). https://doi.org/10.1016/S0921-5093(01)01295-3.
43. J. Heijboer, *Modulus and Damping of Polymers in Relation to their Structure*, Br. Polym. J. **1** (1), 3-14 (1969). https://doi.org/10.1002/pi.4980010102.
44. M. Vašina, M. Pöschl, P. Zádrapa, *A Study of Significant Factors Affecting Viscoelastic Damping Properties of Polymer Materials*, Manuf. Technol. **18** (3), 523-529 (2018). https://doi.org/10.21062/ujep/132.2018/a/1213-2489/MT/18/3/523.
45. D. Halliday, R. Resnick, J. Walker, *Fundamentals of Physics*, Extended, 10th Edition. John Wiley & Sons, New York, USA, 2014.
46. V. Rievaj, O. Stopka, J. Vrábel, L. Mokrickova, C. Schmidt, *The Impact of Air Resistance on the Fuel Consumption in Real Conditions within the Transport Operation*, Commun. Sci. Lett. Univ. Zilina **18** (2), 57-61 (2016). DOI: 10.26552/com.C.2016.2.57-61.
47. Z. Trojanová, P. Lukáč, J. Džugan, K. Halmešová, *Amplitude Dependent Internal Friction in a Mg-Al-Zn Alloy Studied after Thermal and Mechanical Treatment*, Metals **7 (10)**, 433 (2017). https://doi.org/10.3390/met7100433.
48. I.S. Golovin, *Damping Mechanisms in High Damping Materials*, Key Eng. Mater. **319**, 225-230 (2006). https://doi.org/10.4028/www.scientific.net/kem.319.225.
49. D.E. Kretschmann, *Mechanical Properties of Wood*, (ch. 5), in: General Technical Report FPL-GTR-190: Wood Handbook-Wood as an Engineering Material. Department of Agriculture, Forest Service, Forest Products Laboratory, Madison, WI, USA, 2010.
50. E.-S. Jang, C.-W. Kang, *Sound Absorption Characteristics of Three Species (Binuang, Balsa and Paulownia) of Low Density Hardwood*, Holzforschung **75** (12), 1115-1124 (2021). https://doi.org/10.1515/hf-2021-0049.
51. R. Viala, V. Placet, S. Cogan, *Simultaneous Non-destructive Identification of Multiple Elastic and Damping Properties of Spruce Tonewood to Improve Grading*, J. Cult. Herit. **42**, 108-116 (2020). https://doi.org/10.1016/j.culher.2019.09.004.
52. J. Göken, S. Fayed, H. Schäfer, J. Enzenauer, Acta Phys. Pol. A **133** (5), 1241-1260 (2018). DOI: 10.12693/APhysPolA.133.1241.
53. E. Rohloff, *Über die innere Reibung von Geigenholz*, Z. Physik **117**, 64-66 (1941). https://doi.org/10.1007/BF01337409.
54. A. Granato, K. Lücke, *Theory of Mechanical Damping Due to Dislocations*, J. Appl. Phys. **27** (6), 583-593 (1956). https://doi.org/10.1063/1.1722436.
55. H. Becker, D. Noack, *Studies on Dynamic Torsional Viscoelasticity of Wood*, Wood Sci. Technol. **2**, 213-230 (1968). https://doi.org/10.1007/BF00350910.
56. A.-M. Olsson, L. Salmén, *The Association of Water to Cellulose and Hemicellulose in Paper Examined by FTIR Spectroscopy*, Carbohydr. Res. **339** (4), 813-818 (2004). https://doi.org/10.1016/j.carres.2004.01.005.
57. E.T. Engelund, L.G. Thygesen, S. Svensson, C.A.S. Hill, *A Critical Discussion of the Physics of Wood-Water Interactions*, Wood Sci. Technol. **47**, 141-161 (2013). https://doi.org/10.1007/s00226-012-0514-7.